Research Square

Preprints are preliminary reports that have not undergone peer review.
They should not be considered conclusive, used to inform clinical practice,
or referenced by the media as validated information.

H2S Exposure Aggravates Inflammation Induced by LPS in Chicken Liver By microRNA-216a/PKCα Axis Modulating NF-κB/TNFα Pathway

Jinming Guo
Northeast Agricultural University
Wenjing Zhu
Northeast Agricultural University
Yilin Yin
Northeast Agricultural University
Xu Shi
Northeast Agricultural University
Shi-wen Xu (shiwenxu@neau.edu.cn)
Northeast Agricultural University

Research

Keywords: H2S, Liver tissue, LPS, Necrosis and Pyroptosis, Inflammation

Posted Date: November 3rd, 2021

DOI: https://doi.org/10.21203/rs.3.rs-998778/v1

License: This work is licensed under a Creative Commons Attribution 4.0 International License.
Read Full License

H_2S exposure aggravates inflammation induced by LPS in chicken liver by microRNA-216a/PKCα axis modulating NF-κB/TNFα pathway

Jin-ming Guo[a], Wen-jing Zhu[a], Yi-lin Yin[a], Xu Shi[a], Shi-wen Xu[a, b,*]

[a] College of Veterinary Medicine, Northeast Agricultural University, 600 Changjiang Road, Harbin 150030, P. R. China

[b] Key Laboratory of the Provincial Education Department of Heilongjiang for Common Animal Disease Prevention and Treatment, College of Veterinary Medicine, Northeast Agricultural University, Harbin, 150030, PR China.

* Corresponding author. College of Veterinary Medicine, Northeast Agricultural University, Harbin, 150030, P. R. China.

E-mail addresses: shiwenxu@neau.edu.cn (S. Xu)

Address: College of Veterinary Medicine, Northeast Agricultural University, Harbin, 150030, P. R. China (Shiwen Xu)

Tel: +86 0451 55190407

Abstract

Background: Hydrogen sulfide (H_2S), a common air pollutant and toxic gas, which is harmful to organisms and the environment. Exposure to high concentrations of H_2S can lead to necrosis and inflammation. However, the potential mechanism of H_2S-induced hepatotoxicity and the role of microRNA (miRNA) in this process are still poorly understood. In this experiment, 80 one-day-old chickens were used as model organisms to evaluate the effects of H_2S and Lipopolysaccharide (LPS) on poultry liver. Four groups (Control group, LPS group, H_2S group, H_2S-LPS group) were established. Liver tissue was collected after 42 days of age. Ultrastructural observation, pathological tissue observation, immunofluorescence analysis, real-time quantitative PCR analysis and Western blot analysis were used to detect.

Results: The results showed that obvious pyroptosis was observed in ultrastructure. Histopathological observation showed obvious necrosis and inflammatory injury in broiler liver tissue. By detecting the expression of miR-216a in the four groups, we verified that miR-216a can target chicken PKCα. Molecular level studies showed that H_2S exposure could inhibit the expression of miR-216a, promote the up-regulation of PKCα, activate the NF-κB/TNFα signaling pathway, induce cell necrosis (necrosis marker factors RIP1, RIP3, caspase8, MLKL, NLRP3) and pyroptosis-related gene expression (ASC, caspase1, GSDMD), and eventually lead to inflammatory injury of chicken liver (IL-1β, IL-6, IL-18, iNOS).

Conclusions: We concluded that H_2S induced the imbalance of the NF-κB/TNFα signaling pathway through miR-216a/PKCα axis, leading to chicken liver necrosis and cell pyroptosis, and further causing inflammatory injury. Notably, we also found that H_2S aggravated LPS-induced liver inflammation. This study can provide reference to the pathological mechanism of animal damage and poultry poisoning caused by H_2S pollution in the atmospheric environment.

Keywords:H_2S; Liver tissue; LPS; Necrosis and Pyroptosis; Inflammation.

1. Introduction

Hydrogen sulfide (H_2S) is a colorless, poisonous pollutant[1], and one of the ingredients of haze pollution[2]. Environment pollution induced by H_2S is causing concerns among human beings. With the acceleration of industrialization, there is a large amount of H_2S emitted in industrial production and daily life, such as petroleum refineries and coal, sulfuric acid, dyes and cosmetics[3], paper mills, wastewater treatment plants, and landfills. In modern poultry farms, H_2S is also a common noxious gas. Sulfur-containing organic matter in accumulated feces is decomposed under anaerobic conditions and reduced by bacterial sulfate to form hydrogen sulfide gas. H_2S exposure at a low concentration may cause headache, fatigue, nausea[4]. The high concentration of H_2S will adversely affect the normal growth and reproduction of poultry. In 2011, studies reported negative effects of atmospheric H_2S on broiler farming, the growth performance and meat quality of broilers have decreased significantly[5]. In recent years, reports on H_2S damage to poultry have gradually increased. For example, H_2S can cause serious damage to the respiratory system, circulatory system, digestive system, motor system, reproductive system and immune system of poultry. It has been reported that high concentration of H_2S exposure induces tracheal necrosis and apoptosis in broilers through lncRNA3037/miR-15 targeting A20 and BCL2[6]. H_2S can cause energy metabolism via AMPK/HIF-a pathway and induced hepatocyte apoptosis[7]. The high concentration of H_2S gas in chicken houses caused the overexpression of mitochondrial fission genes (Drp1 and Mff) and the weakening of ATPase activity, resulting in mitochondrial structural damage, reduced energy metabolism and myocardial cell apoptosis[8]. H_2S can induce redox homeostasis disorder in broiler jejunum through differential expression of CYP450s, resulting in inflammatory response, immune dysfunction and apoptosis[9]. H_2S in the atmosphere aggravates the imbalance of Th1/Th2, activates inflammatory factor NF-κB and regulates insulin-like growth factor (IGF) signaling pathway-related factors, resulting in glucose metabolism disorder and bone inflammation in broilers[10]. It has also been reported that chronic H_2S irritation at low level can lead to detrimental effects on animal reproduction[11]. H_2S exposure initiates JNK/MST1/FOXO1 pathway and causes immune dysfunction and death in chicken breast cells.[12]

MicroRNAs (miRNAs), first discovered in 1983, are small[13], single-stranded, endogenous non-coding RNAs around 19-24 nucleotides[14]. miRNAs bind to their 3′-untranslated region (3′-

UTR) to negatively modulate expression of target mRNAs, further modulate some biological reactions[15] [16] [17] [18]. For example, previous studies confirmed that the long coding RNA LINC00339 could activate NLRP3 via miR-22-3p, and further induce the pyroptosis of renal tubular epithelial cells in calcium oxalate nephropathy patients[19]. It has been shown that RNA MALAT1 could activate NLRP3 and promote hyperglycemic pyrotosis of renal tubular epithelial cells by inhibiting miR-23c expression[20]. Research showed that overexpression of miR-200a-3p could aggravate inflammation in brain injury caused by sepsis through NLRP3[21]. A study indicated that the increase of miR-34a expression can cause the increase of IL-1β mRNA expression, which may be an essential factor in inducing chronic inflammation in osteoarthritis cartilage tissues[22]. MicroRNA-216a is a member of the miR-216 family, which is extensively expressed in different species[23]. It is reported that overexpression of miR-216a caused increase of the expression of Bax and p53 in MCF-7 cells, which indicated miR-216a caused apoptosis[24]. miR-216a can reduce the genesis of tumour and blood vessel in breast cancer cells by targeting the 3′-UTR of CD4430[23]. Yang et al. have reported that miR-216a could accelerate inflammation and senescence of endotheliocyte by targeting Smad3 and thereafter regulate NF-κB signaling[25].

Inflammatory gene expression is regulated by many transcription factors, including NF-κB and TNF-α. Interleukin (IL)-1β and IL-6[26] are both critical proinflammatory cytokines[27]. NO, which is produced by iNOS, has a wide range of physiological and pathophysyologic effects and plays an essential role in the development of inflammation and tumor [28]. In addition to NO and ROS levels, also TNF-α, IL-6, and IL-1β will be released in LPS-stimulated macrophages via the NF-κB pathway[29]. Necrosis, a type of non-apoptotic programmed cell death, is characterized by the release of pro-inflammatory cellular components through membrane lysis, inducing an inflammatory response[30], and the kinases receptor-interacting protein 1 (RIP1) and receptor-interacting protein kinase3 (RIP3) are pivotal signaling molecules in necrotic cell death[31]. Mixed lineage kinase domain-like protein (MLKL) is an important downstream component[32] mediated by RIP3[33] in inflammasome signaling and TNF-induced (Tumor necrosis factor, TNF) necrosis[34]. Activation of RIP3 can induce NLRP3 inflammatory pathways and necroptosis activation[35]. Pyroptosis, a programmed cell death. And as an important target of pyroptosis related pathway, NLRP3 could induce pyroptosis when activated[36] GSDMD, as one of the major factors

in the GSDM family, plays a crucial role in regulating the process of pyroptosis[36]. Caspase-1, the key factors of pyroptosis, can recruit NLRP3 and ASC to form NLRP3 inflammatory small body complex. The ion gradient on both sides of the cell membrane is unbalanced, resulting in cell swelling and cell membrane rupture[37]. The preIL-18 of the preIL-1 band is processed into an activated secretory form, releasing pro-inflammatory factors, namely pyroptosis, and further initiating inflammatory immune response in the host[38]. GSDMD plays a central role in the release of the pro-inflammatory cytokine IL-1β, suggesting that there is a relationship between the key factors of pyrogen death and inflammation[39] Activating caspase-8 can lead to cell membrane damage and K^+ outflow, which leads to the activation of NLRP3 inflammasomes and triggers post-ASC oligomerization. Furthermore, it has also been found that inflammation is closely related to caspase-8-mediated pyroptosis[40].

In recent years, there has already been some researches about high concentration of H_2S in the environment can cause damages to different organs and tissues. It has been confirmed that the existence of a targeted relationship between miR-216a and PKCα, however, the mechanism of H_2S exposure to hepatotoxicity in chickens and the involvement process of miR-216a is still unclear. For this purpose, we chose the liver of chicken as the model and built the model of H_2S poisoning and LPS treatment of the chicken in vivo. We collected livers of chicken to observe hematoxylin eosin stain (HE stain). Real-time quantitative PCR (qRT-PCR) and Western blotting detection were performed in vivo to examine the expressions of miR-216a, necrosis, pyroptosis and inflammation related genes in the liver during exposure to H_2S gas. Our results suggested H_2S exposure caused liver necrosis and pyroptosis in chickens by inducing the NF-κB/TNFα pathway mediated by the miR-216a/PKCα axis and aggravated the inflammation caused by LPS. Studies like this may help better understanding how toxic gases such as H_2S in the atmosphere can have adverse effects on animals living in polluted terrestrial environments.

2. Materials and methods

2.1 Animals feeding and treatment

All the procedures used in our study were approved by the Institutional Animal Care and Use Committee of the Northeast Agricultural University. 80 one-day-old broilers were divided into two groups randomly, each group was 40 broilers named the Control group and H_2S group. Each group

was fed in a separate room, ingestion and drinking were optional. Temperature, indoor humidity, CO_2 concentration, air velocity and other environmental parameters were stationary and appropriate. H_2S concentration was administered according to **Table 1**. At 42 days old, we chose 20 broilers from the Control group stochastically, named LPS group. Analogously, we chose 20 broilers from H_2S group randomly, denominate is H_2S-LPS group. LPS group and H_2S-LPS group received intraperitoneal injection with LPS (0.2μg /kg) for 5 hours and the 4 groups broilers were euthanized. The liver tissue samples of four groups were collected for further use.

2.2 Microscopic examination of liver

The liver tissue was taken out and fixed with 2.5% glutaraldehyde, washed three times with PH 7.2 phosphate buffer, 15 min each time. 1% osmic acid was fixed and rinsed again. After gradient ethanol dehydration, the embedded samples were soaked in uranium acetate-lead citrate double staining and observed under electron microscope.

2.3 Hematoxylin and Eosin (H & E) observation

Sections of the obtained liver tissue were placed in 10% neutral formalin for fixation for at least 24 hours and then dehydrated with alcohol. The slices of liver tissue embedded with paraffin wax, and sectioning to a proper thickness of about 5μm, stained with hematoxylin and eosin, and observed under light microscope.

2.4 Immunofluorescence analysis of liver

Paraffin section dewaxing, serum blocking for 30 min. Primary antibodies GSDMD (1:200, Abclone, USA) and NLPR3 (1:200, wanleibio, China) were incubated overnight at 4 ℃. The secondary antibody was incubated at room temperature for 50 min. Spontaneous fluorescence quenching agent was added and washed with PBS. Observation under fluorescence microscope.

2.5 RNA extraction and qRT-PCR detection of liver tissue

2.5.1 RNA extraction from liver tissue

Grind 0.1g liver tissue completely in liquid nitrogen, add 1ml Trizol solution and mix well into a 1.5ml EP tube. After adding 400 μL of chloroform, shake vigorously and mix well, and let stand for 5 min. After the precipitation is separated, centrifuge at 12000g at 4°C for 15 min, and gently aspirate 300 μL of the supernatant. After adding 300 μL of isopropanol, turn gently, mix well, let stand at room temperature for 8 minutes, 4°C, 12000g, centrifuge for 10 minutes, discard the supernatant, and save the precipitate. Add 1000μL of DEPC ethanol (75%), gently pipette until

completely dissolved at 4°C, 10000g, centrifuge for 10min, discard the supernatant, keep the precipitate, and dry at room temperature for 5min. Add 40μl of DEPC water until it is evenly mixed, and determine the concentration and purity of RNA for reverse transcription.

2.5.2 cDNA synthesis of liver tissue

The reaction system was prepared according to the manufacturer's instructions. The mixed system was sealed, it was taken out and stored at -20°C for later use after the reaction was completed. Reverse transcription of miRNAs was performed by the microRNA First chain cDNA Synthesis Kit (Tien Biotechnology Co., LTD., Beijing), and RT-PCR was performed on LightCycler®480 II detection system (Roche, Switzerland). Description of microRNA (http://mirdb.org/) gga-miR-216a and target gene PKCα was shown in **Fig.1A**. TargetScan database (http://www.targetscan.org/) predicts that binding sites for miRNA-216a, and the targeting site located at 624 to 630 bp in the 3′-UTR of PKCα, as shown in **Fig.1B**.

2.5.3 Detection of mRNA expression of related genes in liver tissue by qRT-PCR method

The DNA obtained by the reaction was configured according to the reaction solution system in **Table 2**, and fluorescence quantitative detection was performed. The primer sequences are shown in **Table 3**. qRT-PCR uses LightCycler®480 system (Roche, Basel, Switzerland) and Fast Universal SYBR Green Master Mix (Roche, Basel, Switzerland). The mRNA relative levels was calculated by $2^{-\triangle\triangle Ct}$.

2.6 The protein of liver tissue was extracted and detected by Western blot

Western blot is used to detect the protein levels of necrosis, pyroptosis and inflammation-related genes. The protein from liver tissue was separated by electrophoresis. Transfer the protein to the PVDF membrane for 90 minutes under low temperature conditions. The membrane was blocked with 5% skim milk at 37°C for 2 hours, and then incubated with the primary antibody for 12 hours at 4°C. After washing three times with PBST for 15 minutes, the membrane was incubated with the secondary antibody of rabbit IgG for 1 hour at room temperature. Use X-ray film to detect the signal. Rabbit polyclonal antibody was used to analyze the content of β-actin as a loading control. Use Image J to calculate the optical density (OD) of the protein bands.

2.7 Statistical analysis

Statistical analysis was performed using GraphPad Prism (version 7.0, GraphPad Software Inc.,

San Diego, CA, USA) with one-way ANOVA with Turkey's test. All experiments were performed in three repetitions. All data show normal distribution and pass the equal variance test, and are expressed as mean ± standard (SD). Different letters represent significant differences. Data differences are considered statistically significant when $P<0.05$.

3. Results

3.1 Observation of the pathological structure of liver tissue

The liver tissue of the Control group is shown in **Fig.2A**: the liver cells are tightly arranged, the morphology is normal, and the nucleolus is clear. The liver lobules are structurally complete and have normal physiological morphology. The hepatocyte cords are arranged neatly, the cells are evenly stained, and the liver cells have no obvious swelling. However, the tissues of the H_2S group and the LPS group showed typical liver injury characteristics, as shown in **Fig.2B** and **Fig.2C**: Inflammatory cells infiltrate (Black arrows), unclear cell boundaries, the nuclear were karyolysis and disappeared (Red arrows), liver cells are relatively loosely arranged, and cell edges are blurred. The arrangement of hepatocyte cords is disordered, and hepatic sinusoids are obviously dilated and congested. Compared with the H_2S group and the LPS group, the damage of the H_2S-LPS group was more serious, the intercellular space was significantly enlarged, the cell structure was more blurred, and the inflammatory cell infiltration phenomenon was more obvious, as shown in **Fig.2D**.

3.2 Observation of the histopathological changes of liver tissue

As shown in **Fig.3A**, the cell morphology of the Control group was normal, and the nucleus was approximately round without obvious pathological changes (Blue boxes). **Fig.3B** and **Fig.3C**, the H_2S group and LPS group, hepatocyte mitochondrial cristae rupture. At the same time, typical pathological changes of cell pyroptosis occurred: mitochondria swelled and vacuolated, holes formed on the cell membrane, cytoplasmic contents overflowed (Red boxes), and a large number of vacuoles (Yellow boxes) were formed. In the H_2S-LPS group, as shown in **Fig.3D**, pathological changes with pyroptosis were more significant.

3.3 H_2S exposure increases expression of NLRP3 and GSDMD in chicken liver

The cells in the Control group were normal (Blue) as shown in **Fig.4A**. Green (GSDMD) and red (NLRP3) cells were found in **Fig.4B** and **Fig.4C**, and the cells with increased expression of GSDMD and NLRP3 were yellow (Red arrows). Fluorescence staining analysis showed that the

expressions of NLRP3 and GSDMD increased in H_2S group and LPS group. **Fig.4D** showed the most pyroptosis cells, indicating that the pyroptosis phenomenon was the most obvious in the H_2S-LPS group.

3.4 H_2S exposure changes the expression pattern of microRNA-216a/PKCα axis

As shown in **Fig.1C**, the expression of microRNA-216a and PKCα in liver tissue was detected by qRT-PCR. We found that H_2S exposure could inhibit the expression of microRNA-216a. On the contrary, H_2S exposure significantly increased the expression level of PKCα at the mRNA and protein levels. The above results indicated that H_2S exposure significantly changed the expression pattern of microRNA-216a/PKCα axis in chicken liver.

3.5 H_2S induces chicken liver necrosis and pyroptosis by activating NF-κB/TNFα pathway

As shown in **Fig.5**, compared to the Control group, the expression levels of NF-κB and TNFα mRNA (**Fig.5A**) and protein (**Fig.5B**) in the H_2S exposure environment were significantly increased. Compared with the LPS group and the H_2S group, the expression levels of NF-κB and TNFα in the H_2S-LPS group were more significant. These data suggested that H_2S exposure activated NF-κB / TNFα pathway. At the same time, we found that the mRNA (**Fig.6A**) and protein (**Fig.6C**) levels of RIP1, RIP3, MLKL and NLRP3 in H_2S and LPS groups were significantly increased, and the mRNA and protein expression levels of caspase8 was decreased. The expression of necrosis related genes in H_2S-LPS group changed more obviously.

The mRNA (**Fig.6B**) and protein (**Fig.6C**) expression levels of ASC, caspase1 and GSDMD, the key pyrolysis factors in LPS group and H_2S group, were also significantly higher than those in Control group. Similarly, the expression of pyroptosis-related genes in H_2S-LPS group was more significant than that in LPS group and H_2S group. The above resulted show that H_2S activates NF-κB/TNFα pathway to induced liver necrosis and pyroptosis, and also aggravated LPS-induced pyroptosis in liver tissue.

3.6 Inflammatory injury of liver tissue induced by H_2S exposure

As shown in **Fig. 7A**, IL-1β and IL18, IL-6 and iNOS, as the key factors of inflammation, were significantly increased at the mRNA level. When exposed to H_2S, the protein expression levels of IL-1β, IL-6 and iNOS were significantly increased, as shown in **Fig. 7B**. Similarly, the expression

levels of these factors were significantly increased after LPS treatment. Compared with H_2S group and LPS group, the expression level of key inflammatory factors in H_2S-LPS group was significantly increased. The above results showed that H_2S exposure caused inflammation in chicken liver tissue and aggravated LPS-induced liver inflammation.

4. Discussion

H_2S is a major pollutant in the air and has negative effects on human beings and different kinds of animals[41], it causes damage to different tissues and organs in complex and diverse mechanism of toxicity. At present, the reports have documented that high concentration H_2S exposure in the air can induce damages in poultry. For example, studies have shown that H_2S exposure can induce the FOS/IL8 signaling pathway mediated by oxidative stress, and cause the inflammatory injury of chicken trachea[42]. Previous studies have shown that H_2S cause inflammatory reaction by CYP450s differential expression in chicken jejunum tissue[9]. In this experiment, we illuminated that H_2S exposure decreased miR-216a expression. H_2S exposure induced chicken liver necrosis and pyroptosis through NF-κB/TNFα pathway mediated by miR-216a/PKCα axis, and ultimately induced inflammation. H_2S aggravated LPS-induced necrosis and pyroptosis, further aggravating inflammatory injury.

Studies have shown that H_2S exposure could change the expression of microRNA. For example, the miR-15b-5p/TGFBR3 axis regulates H_2S-induced broiler bursal necrosis and inflammation[43]. Studies indicated that miR-216a can regulate necrosis and inflammation. For instance, studies have shown that Cd activates oxidative stress and miR-216a-PI3K/AKT axis disorders, thereby promoting lymphocyte apoptosis and necrosis [44]. miR-216a reduced LPS-induced inflammatory damage by regulating JAK2/STAT3 and NF-κB signaling pathways [45]. Studies have found that miR-216a significantly inhibited inflammatory mediators after oxygen and glucose deprivation, including inflammatory enzymes (iNOS and MMP-9) and cytokines (TNFα and IL-1β). Up-regulating miR-216a levels could reduce ischemic infarction and improve neurological deficits [46]. According to the prediction results on the TargetScan website, as shown in the **Fig.1**. We found that miR-216a targeted PKCα in chickens. The 3′-UTR site of PKCα bound on miR-216a in mammals, such as human, chimp, rhesus, cat and dog, has the same nucleotide sequence as chicken. Cui et al. have discovered that dual-luciferase reporter assay confirmed that miR-216a can target directly

PKCα[47]. The results of this experiment showed that the expression of miR-216a decreased and the expression of PKCα increased in the H_2S group, which verified the relationship of miR-216a targeting PKCα in the species chicken and illustrated miR-216a is involved in the toxicity of H_2S. This targeting relationship has been consistently verified in our experiments. These results indicated that the regulatory relationship of miR-216a/PKCα has been discovered in chickens.

Studies have reported that PKCα could activate NF-κB (p65) and played a key role in activation of inflammatory response[48]. TNFα can induce activation of NF-κB, TNFα also be activated by NF-κB[49]. Both of them are key factors of activating necrosis and inflammatory pathways[50] [51] [52], can cause activation of RIP1 to induce necrocytosis by RIP1-RIP3 pathway and lead to inflammation eventually [53]. Our research showed exposure to H_2S could inhibit the expression of miR-216a, leading to up-regulation of PKCα expression, thereby activating the NF-κB/TNFα pathway. Pathological observation showed typical changes of cell necrosis in liver exposed to H_2S: the nuclear were karyolysis and cytoplasmic disintegration. Therefore, we further verified the key factors of necrosis. Our results showed that compared with the Control group, the expression of NF-κB, TNF-α, RIP1, RIP3 and MLKL in the H_2S group increased significantly at the mRNA and protein levels. And the expression of caspase8, a key factor of necrosis, was significantly decreased compared with the Control group, indicating that H_2S through miR-216a/PKCα axis activated NF-κB/TNFα pathway and induced hepatocyte necrosis. Previous researches studies have involved H_2S exposure induced pyroptosis in the trachea of broilers via the regulatory effect of circRNA-17828/miR-6631-5p/DUSP6 crosstalk on ROS production[54]. Our ultrastructure observation results showed that under the condition of H_2S gas exposure, there were typical pyroptosis features of cells: cell rupture, content logistics, blurred or ruptured cell edge. It hinted that H_2S exposure caused cell pyroptosis. For further verification, the results of immunofluorescence staining were consistent with those of ultrastructure observation. For this reason, we examined whether the expression level of pyroptosis related genes changed under H_2S stimulation. The results showed that compared with the Control group, the expression of ASC, caspase1 and GSDMD changed significantly in the H_2S group, At the same time, it indicated that H_2S exposure caused liver pyroptosis. It's been documented that one of the important mechanisms caused by LPS is NF-κB signaling pathway[55]. Studies have shown that LPS could activate NLRP3 inflammasome [56].

The study has demonstrated that repurified LPS could activate the caspase-1/IL-1β pathway during acute kidney failure, leading to pyroptosis [57]. Similarly, our experimental results showed that compared with the Control group, the expression of NF-κB/TNFα gene and genes related to necrosis and pyrogenesis in LPS group were significantly changed at mRNA and protein levels. It was suggested that LPS activated the NF-κB/TNFα pathway, leading to necrosis and pyroptosis of the RIP1-RIP3 pathway in chicken liver. Compared with LPS group, the changes of the above indexes in H_2S-LPS group were more significant, indicating that H_2S caused liver necrosis and pyroptosis, while h H_2S also aggravated LPS-induced liver necrosis and pyroptosis.

Cell necrosis and pyroptosis are two incompletely characterized pro-inflammatory cell death modes. When pro-inflammatory cytokines IL-1β and IL-18 are stimulated and released, these two modes will be activated to promote local and systemic inflammatory responses[58]. We found that H_2S exposure caused liver inflammatory cell infiltration through pathological structure observation, indicating that H_2S exposure caused liver necrosis and pyroptosis eventually led to inflammation. Next, we examined the expression levels of key genes in inflammation. The results showed that the mRNA expression of IL-1β, IL-6, IL18 and iNOS in the H_2S group was significantly higher than that in the Control group, and the protein levels of IL-1β, IL-6 and iNOS also significantly higher. These results indicated that H_2S caused hepatocytes inflammation. These results indicated that H_2S induced liver inflammatory by changing the expression of genes related to necrosis and pyroptosis. The above results indicated that H_2S could cause necrosis and pyroptosis of chicken liver by changing the expression of miR-216a/PKCα axis, and induce inflammation injury eventually. LPS can initiate transcription of genes associated with necrosis signaling[59], and stimulates cells to undergo inflammatory reactions[60]. It have reported that LPS could cause disease symptoms of mastitis in mouse [61]. Compared with LPS group, the expression of H_2S-LPS inflammation-related genes was also significantly increased, suggesting that H_2S aggravated LPS-induced inflammatory injury.

5. Conclusion

In summary, H_2S inhibited the expression of miR-216a and increased the expression of PKCα, which induced chicken liver cell necrosis and pyroptosis by triggering NF-κB / TNFα pathway and further induced inflammatory injury. At the same time, H_2S also aggravated LPS-induced

inflammatory injury of liver tissue. This study not only enriches the research content of H_2S toxicology, but also expands the research direction of H_2S toxicology, and provides reference for comparative medicine (**Fig.8**).

Acknowledgements

I would like to express my heartfelt thanks to all the teachers and students who helped me in the process of completing this paper. I thank my tutor Professor Xu here for providing me with very important suggestions in designing experimental ideas and completing writing. I especially thank the teacher for the encouragement and support that he has given me during my study. Thanks to my classmates for helping me complete data analysis and writing articles. Finally, I want to thank all the teachers and students of the research group, can learn and live in such a mutual help team, is my luck.

Authors' contributions

SWX provided concept research, project design and financial support; JMG, WJZ and YLY performed the experiment; JMG and WJZ contributed significantly to analysis and manuscript preparation; JMG, WJZ and XS performed the data analyses and wrote the manuscript; WJZ and XS helped perform the analysis with constructive discussions. All authors read and approved the final manuscript.

Funding

The study was supported by the National Key Research and Development Program of China (No. 2016YFD0500501) and China Agriculture Research System (CARS-41–17).

Availability of data and materials

The datasets generated for this study are available upon request to the corresponding author.

Declarations

Ethics approval and consent to participate

All procedures performed in this study were approved by the Institutional Animal Care and Use Committee of Northeast Agricultural University (SRM-11).

Consent for publication

The author confirm:

The work described has not been published before (except in the form of a summary or as part of a lecture, comment or paper published); It does not consider publishing elsewhere; Its publication has been approved by all co-authors; The publication of this article has been approved (either implicitly or explicitly) by the Northeast Agricultural University.

Competing interests

The authors declare that they have no known competing financial interests or personal relationships that could have appeared to influence the work reported in this paper.

Author details

[a] College of Veterinary Medicine, Northeast Agricultural University, 600 Changjiang Road, Harbin 150030, P. R. China

[b] Key Laboratory of the Provincial Education Department of Heilongjiang for Common Animal Disease Prevention and Treatment, College of Veterinary Medicine, Northeast Agricultural University, Harbin, 150030, PR China.

Reference

1. Lashgari M, Ghanimati M. An excellent heterojunction nanocomposite solar-energy material for photocatalytic transformation of hydrogen sulfide pollutant to hydrogen fuel and elemental sulfur: A mechanistic insight. Journal of Colloid and Interface Science. 2019;555:187–94.

2. Chen C, Xu D, He MZ, Wang Y, Du Z, Du Y, et al. Fine Particle Constituents and Mortality: A Time-Series Study in Beijing, China. Environmental Science & Technology. 2018;52:11378–86.

3. Yan Y, Zhang K, Yu H, Zhu H, Sun M, Hayat T, et al. Sensitive detection of sulfide based on the self-assembly of fluorescent silver nanoclusters on the surface of silica nanospheres. Talanta. 2017;174:387–93.

4. Locateli Godoi AF, Grasel AM, Polezer G, Brown A, Potgieter-Vermaak S, Scremim DC, et al. Human exposure to hydrogen sulphide concentrations near wastewater treatment plants. Science of the Total Environment. 2018;610:583–90.

5. Y. Wang, M. Huang, Q. Meng, and Y. Wang. Effects of atmospheric hydrogen sulfide concentration on growth and meat quality in broiler chickens. Poultry Science. 90:2409–2414.

6. Li X, Chen M, Shi Q, Zhang H, Xu S. Hydrogen sulfide exposure induces apoptosis and necroptosis through lncRNA3037/miR-15a/BCL2-A20 signaling in broiler trachea. Science of The Total Environment. 2020;699:134296.

7. Guo J, Xing H, Chen M, Wang W, Zhang H, Xu S. H2S inhalation-induced energy metabolism disturbance is involved in LPS mediated hepatocyte apoptosis through mitochondrial pathway. Science of the Total Environment. 2019;663:380–6.

8. Hydrogen sulfide-induced oxidative stress leads to excessive mitochondrial fission to activate apoptosis in broiler myocardia.

9. Zheng S, Jin X, Chen M, Shi Q, Zhang H, Xu S. Hydrogen sulfide exposure induces jejunum injury via CYP450s/ROS pathway in broilers. Chemosphere. 2019;214:25–34.

10. Jing H, Gao X, Xu L, Lin H, Zhang Z. H2S promotes a glycometabolism disorder by disturbing the Th1/Th2 balance during LPS-induced inflammation in the skeletal muscles of chickens. Chemosphere. 2019;222:124–31.

11. Lewis RJ, Copley GB. Chronic low-level hydrogen sulfide exposure and potential effects on human health: A review of the epidemiological evidence. Critical Reviews in Toxicology. 2015;45:93–123.

12. Qianru Chi a, Xueyuan Hu a, Zhaoyi Liu a, Yanfei Han a, Dayong Tao b, Shiwen Xu a,b, Shu Li a,. H2S exposure induces cell death in the broiler thymus via the ROS-initiated JNK/MST1/FOXO1 pathway. Ecotoxicology and Environmental Safety.

13. Su XW, Lu G, Leung CK, Liu Q, Li Y, Tsang KS, et al. miR-181d regulates human dendritic

cell maturation through NF-B pathway. Cell Proliferation. 2017;50:e12358.

14. Bartel DP. MicroRNAs: Genomics, biogenesis, mechanism, and function (Reprinted from Cell, vol 116, pg 281-297, 2004). Cell. 2007;131:11–29.

15. Zhao X, He W, Li J, Huang S, Wan X, Luo H, et al. MiRNA-125b inhibits proliferation and migration by targeting SphK1 in bladder cancer. American Journal of Translational Research. 2015;7:2346–54.

16. Gao Y, Xue Q, Wang D, Du M, Zhang Y, Gao S. miR-873 induces lung adenocarcinoma cell proliferation and migration by targeting SRCIN1. American Journal of Translational Research. 2015;7:2519–26.

17. Jing W, Jiang W. MicroRNA-93 regulates collagen loss by targeting MMP3 in human nucleus pulposus cells. Cell Proliferation. 2015;48:284–92.

18. Li Z, Yu X, Shen J, Liu Y, Chan MTV, Wu WKK. MicroRNA dysregulation in rhabdomyosarcoma: a new player enters the game. Cell Proliferation. 2015;48:511–6.

19. Song Z, Zhang Y, Gong B, Xu H, Hao Z, Liang C. Long noncoding RNA LINC00339 promotes renal tubular epithelial pyroptosis by regulating the miR-22-3p/NLRP3 axis in calcium oxalate-induced kidney stone. Journal of Cellular Biochemistry. 2019;120:10452–62.

20. Li X, Zeng L, Cao C, Lu C, Lian W, Han J, et al. Long noncoding RNA MALAT1 regulates renal tubular epithelial pyroptosis by modulated miR-23c targeting of ELAVL1 in diabetic nephropathy. Experimental Cell Research. 2017;350:327–35.

21. Yu J, Chen J, Yang H, Chen S, Wang Z. Overexpression of miR-200a-3p promoted inflammation in sepsis-induced brain injury through ROS-induced NLRP3. International Journal of Molecular Medicine. 2019;44:1811–23.

22. Yang B, Ni J, Long H, Huang J, Yang C, Huang X. IL-1 beta-induced miR-34a up-regulation inhibits Cyr61 to modulate osteoarthritis chondrocyte proliferation through ADAMTS-4. Journal of Cellular Biochemistry. 2018;119:7959–70.

23. Jeyapalan Z, Deng Z, Shatseva T, Fang L, He C, Yang BB. Expression of CD44 3'-untranslated region regulates endogenous microRNA functions in tumorigenesis and angiogenesis. Nucleic Acids Research. 2011;39:3026–41.

24. Xie Q, Wang S, Zhao Y, Zhang Z, Qin C, Yang X. MicroRNA-216a suppresses the proliferation and migration of human breast cancer cells via the Wnt/beta-catenin signaling pathway. Oncology Reports. 2019;41:2647–56.

25. Yang S, Li J, Chen Y, Zhang S, Feng C, Hou Z, et al. MicroRNA-216a promotes M1 macrophages polarization and atherosclerosis progression by activating telomerase via the Smad3/NF-kappa B pathway. Biochimica Et Biophysica Acta-Molecular Basis of Disease. 2019;1865:1772–81.

26. Jiang S, Yan W, Wang SE, Baltimore D. Dual mechanisms of posttranscriptional regulation of Tet2 by Let-7 microRNA in macrophages. Proceedings of the National Academy of Sciences of the United States of America. 2019;116:12416–21.

27. Wolfrum S, Teupser D, Tan M, Chen KY, Breslow JL. The protective effect of A20 on atherosclerosis in apolipoprotein E-deficient mice is associated with reduced expression of NF-kappa B target genes. Proceedings of the National Academy of Sciences of the United States of America. 2007;104:18601–6.

28. Umesalma S, Sudhandiran G. Differential Inhibitory Effects of the Polyphenol Ellagic Acid on Inflammatory Mediators NF-kappa B, iNOS, COX-2, TNF-alpha, and IL-6 in 1,2-Dimethylhydrazine-Induced Rat Colon Carcinogenesis. Basic & Clinical Pharmacology & Toxicology. 2010;107:650–5.

29. Monica C, Giulio S, Miriam M, Katia F, Paola P, Macri A, et al. In vitro down regulation of proinflammatory cytokines induced by LPS tolerance in pig CD14+cells. Veterinary Immunology and Immunopathology. 2006;112:316–20.

30. Xu F, Luo M, He L, Cao Y, Li W, Ying S, et al. Necroptosis Contributes to Urban Particulate Matter-Induced Airway Epithelial Injury. Cellular Physiology and Biochemistry. 2018;46:699–712.

31. Vandenabeele P, Declercq W, Van Herreweghe F, Vanden Berghe T. The Role of the Kinases RIP1 and RIP3 in TNF-Induced Necrosis. Science Signaling. 2010;3:re4.

32. Zhao J, Jitkaew S, Cai Z, Choksi S, Li Q, Luo J, et al. Mixed lineage kinase domain-like is a key receptor interacting protein 3 downstream component of TNF-induced necrosis. Proceedings of the National Academy of Sciences of the United States of America. 2012;109:5322–7.

33. Vanden Berghe T, Hassannia B, Vandenabeele P. An outline of necrosome triggers. Cellular and Molecular Life Sciences. 2016;73:2137–52.

34. Kang T-B, Yang S-H, Toth B, Kovalenko A, Wallach D. Caspase-8 Blocks Kinase RIPK3-Mediated Activation of the NLRP3 Inflammasome. Immunity. 2013;38:27–40.

35. Guo C, Fu R, Zhou M, Wang S, Huang Y, Hu H, et al. Pathogenesis of lupus nephritis: RIP3 dependent necroptosis and NLRP3 inflammasome activation. Journal of Autoimmunity. 2019;103:102286.

36. Zhang K, Wu Q, Jiang S, Ding L, Liu C, Xu M, et al. Pyroptosis: A New Frontier in Kidney Diseases. Zhou Y, editor. Oxidative Medicine and Cellular Longevity. 2021;2021:1–12.

37. Bolivar, B.E., Vogel, T.P., Bouchier-Hayes, L. Inflammatory caspase regulation: maintaining balance between inflammation and cell death in health and disease. FEBS J 286, 2628–2644.

38. Winkler Stefan., Rösen-Wolff Angela. Caspase-1: an integral regulator of innate immunity. Semin Immunopathol. (2015).37(4), 419-27. doi:10.1007/s00281-015-0494-4.

39. Orning P, Weng D, Starheim K, Ratner D, Best Z, Lee B, et al. Pathogen blockade of TAK1 triggers caspase-8-dependent cleavage of gasdermin D and cell death. Science. 2018;362:1064-+.

40. Sarhan J, Liu BC, Muendlein H, Li P, Nilson R, Tang AY, et al. Caspase-8 induces cleavage of gasdermin D to elicit pyroptosis during Yersinia infection. Proceedings of the National Academy of Sciences of the United States of America. 2018;115:E10888–97.

41. Chi Q, Wang D, Hu X, Li S, Li S. Hydrogen Sulfide Gas Exposure Induces Necroptosis and Promotes Inflammation through the MAPK/NF-kappa B Pathway in Broiler Spleen. Oxidative Medicine and Cellular Longevity. 2019;2019:8061823.

42. Chen M, Li X, Shi Q, Zhang Z, Xu S. Hydrogen sulfide exposure triggers chicken trachea inflammatory injury through oxidative stress-mediated FOS/IL8 signaling. Journal of Hazardous Materials. 2019;368:243–54.

43. Qianru C, Xueyuan H, Bing Z, Qing Z, Kaixin Z, Shu L. Regulation of H2S-induced necroptosis and inflammation in broiler bursa of Fabricius by the miR-15b-5p/TGFBR3 axis and the involvement of oxidative stress in this process. J Hazard Mater. Amsterdam: Elsevier; 2021;406:124682.

44. Zhang J, Zheng S, Wang S, Liu Q, Xu S. Cadmium-induced oxidative stress promotes apoptosis and necrosis through the regulation of the miR-216a-PI3K/AKT axis in common carp lymphocytes and antagonized by selenium. Chemosphere. Oxford: Pergamon-Elsevier Science Ltd; 2020;258:127341.

45. Kong F, Sun Y, Song W, Zhou Y, Zhu S. MiR-216a alleviates LPS-induced acute lung injury via regulating JAK2/STAT3 and NF-kappa B signaling. Hum Cell. Tokyo: Springer Japan Kk; 2020;33:67–78.

46. Tian YS, Zhong D, Liu QQ, Zhao XL, Sun HX, Jin J, et al. Upregulation of miR-216a exerts neuroprotective effects against ischemic injury through negatively regulating JAK2/STAT3-involved apoptosis and inflammatory pathways. J Neurosurg. Rolling Meadows: Amer Assoc Neurological Surgeons; 2019;130:977–88.

47. Cui Y, Wang J, Liu S, Qu D, Jin H, Zhu L, et al. miR-216a promotes breast cancer cell apoptosis by targeting PKC alpha. Fundamental & Clinical Pharmacology. 2019;33:397–404.

48. Lin SB, Wu LC, Huang SL, Hsu HL, Hsieh SH, Chi CW, et al. In vitro and in vivo suppression of growth of rat liver epithelial tumor cells by antisense oligonucleotide against protein kinase C-alpha. Journal of hepatology. 2000;33:601–8.

49. Ruddle NH. Tumor necrosis factor (TNF-alpha) and lymphotoxin (TNF-beta). Current opinion in immunology. 1992;4:327–32.

50. Hsu H, Huang J, Shu HB, Baichwal V, Goeddel DV. TNF-dependent recruitment of the protein kinase RIP to the TNF receptor-1 signaling complex. Immunity. 1996;4:387–96.

51. Ting AT, Pimentel-Muinos FX, Seed B. RIP mediates tumor necrosis factor receptor 1 activation of NF-kappaB but not Fas/APO-1-initiated apoptosis. The EMBO journal. 1996;15:6189–96.

52. Kelliher MA, Grimm S, Ishida Y, Kuo F, Stanger BZ, Leder P. The death domain kinase RIP mediates the TNF-induced NF-kappaB signal. Immunity. 1998;8:297–303.

53. Humphries F, Yang S, Wang B, Moynagh PN. RIP kinases: key decision makers in cell death and innate immunity. Cell Death and Differentiation. 2015;22:225–36.

54. Hydrogen sulfide exposure induces pyroptosis in the trachea of broilers via the regulatory effect of circRNA-17828/miR-6631-5p/DUSP6 crosstalk on ROS production.

55. Han L, Yin K, Zhang S, Wu Z, Wang C, Zhang Q, et al. Dalesconols B inhibits lipopolysaccharide induced inflammation and suppresses NF-kappa B and p38/JNK activation in microglial cells. Neurochemistry International. 2013;62:913–21.

56. Yang J, Zhao Y, Zhang P, Li Y, Yang Y, Yang Y, et al. Hemorrhagic shock primes for lung vascular endothelial cell pyroptosis: role in pulmonary inflammation following LPS. Cell Death Dis. 2016;7:e2363–e2363.

57. Yang C-C, Yao C-A, Yang J-C, Chien C-T. Sialic Acid Rescues Repurified Lipopolysaccharide-Induced Acute Renal Failure via Inhibiting TLR4/PKC/gp91-Mediated Endoplasmic Reticulum Stress, Apoptosis, Autophagy, and Pyroptosis Signaling. Toxicological Sciences. 2014;141:155–65.

58. Brusselle, G.G., Provoost, S., Bracke, K.R., Kuchmiy, A., Lamkanfi, M.,. Inflammasomes in respiratory disease from bench to bedside. Chest 2014 145, 1121–1133.

59. Lipopolysaccharide- induced necroptosis of brain microvascular endothelial cells can be prevented by inhibition of endothelin receptors.

60. Perindopril mitigates LPS-induced cardiopulmonary oxidative and inflammatory damage via inhibition of renin angiotensin system, inflammation and oxidative stress.

61. Jiang A, Zhang Y, Zhang X, Wu D, Liu Z, Li S, et al. Morin alleviates LPS-induced mastitis by inhibiting the PI3K/AKT, MAPK, NF-kappa B and NLRP3 signaling pathway and protecting the integrity of blood-milk barrier. International Immunopharmacology. 2020;78:105972.

Figures

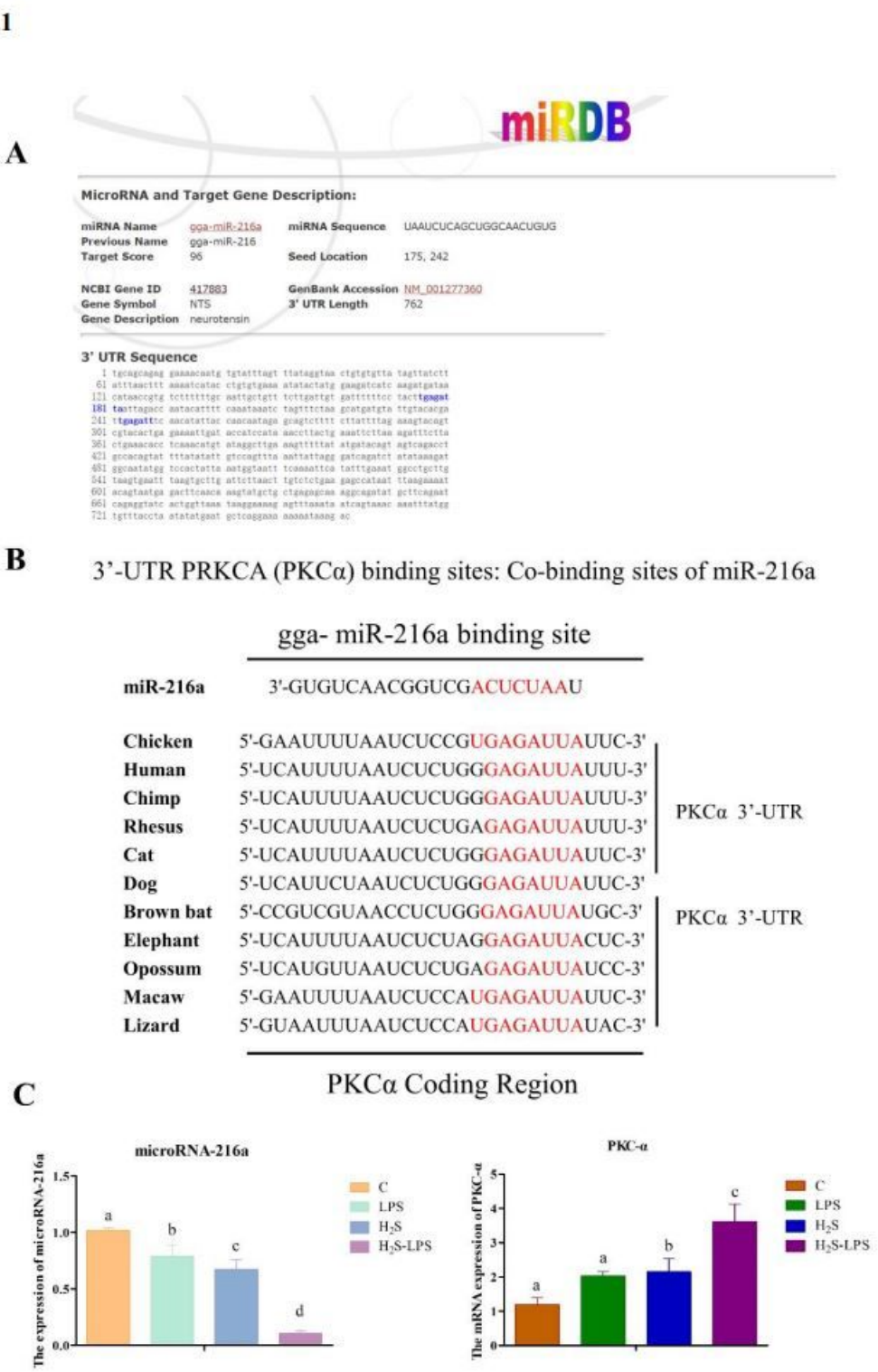

Figure 1

gga-miR-216a directly targets and regulates PKC-α. (A): PKC-α as a predicted target of gga-miR-216a by miRDB (http://mirdb.org/); (B): Prediction results of gene sequences from TargetScan website: Co-binding

sites of miR-216a. (http://www.targetscan.org/); (C): The expressions of microRNA-216a in chicken liver (Left); The mRNA expressions of PKC-α in chicken liver (Right).

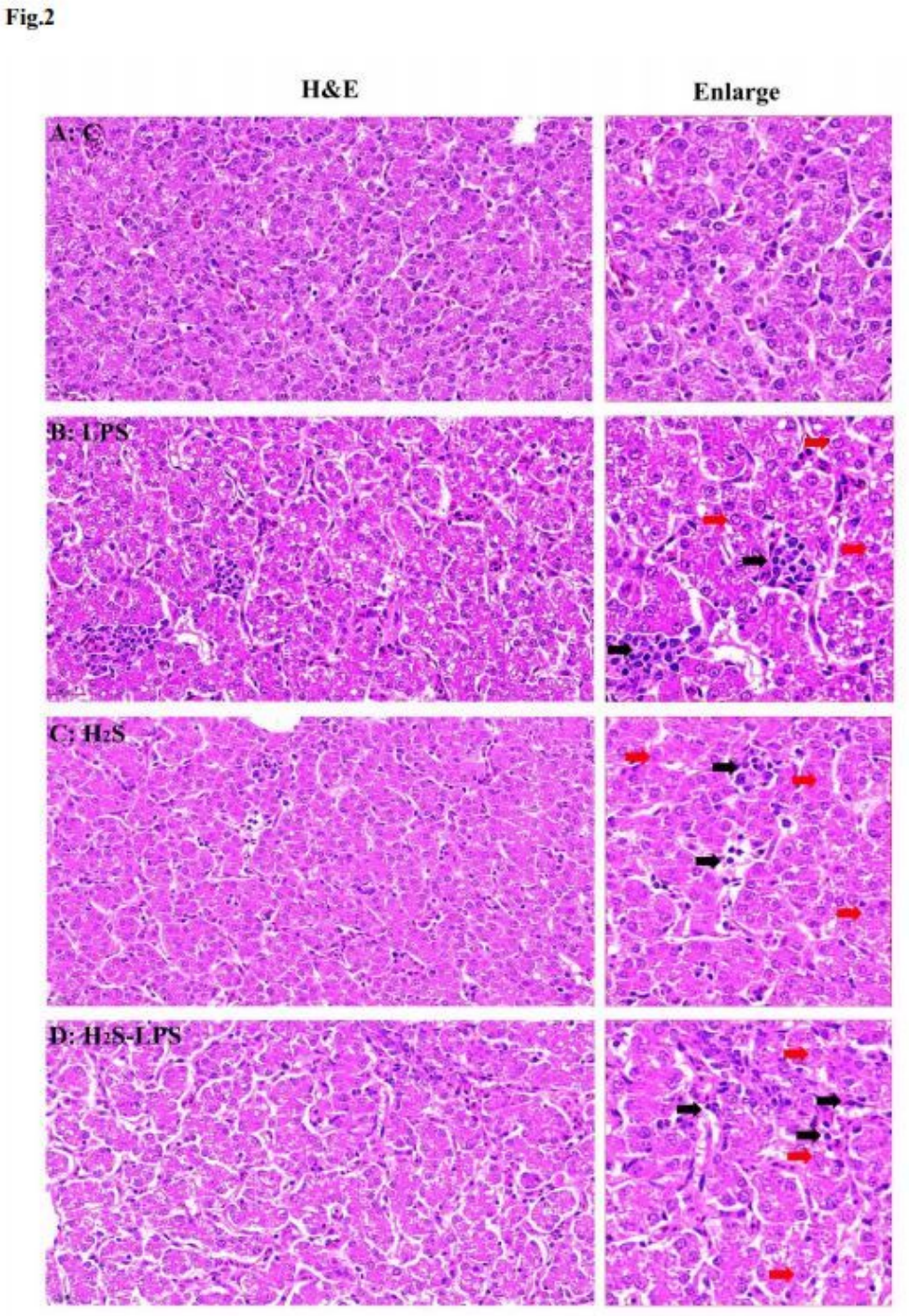

Figure 2

Observation of the histopathological changes of liver tissue. (A): C group; (B): H2S group; (C): LPS group; (D): H2S-LPS group. Fields from one representative experiment of three are shown (Scale bar, 20μm).

Inflammatory cells infiltrate (Black arrows), unclear cell boundaries, the nuclear were karyolysis and disappeared (Red arrows).

Fig. 3

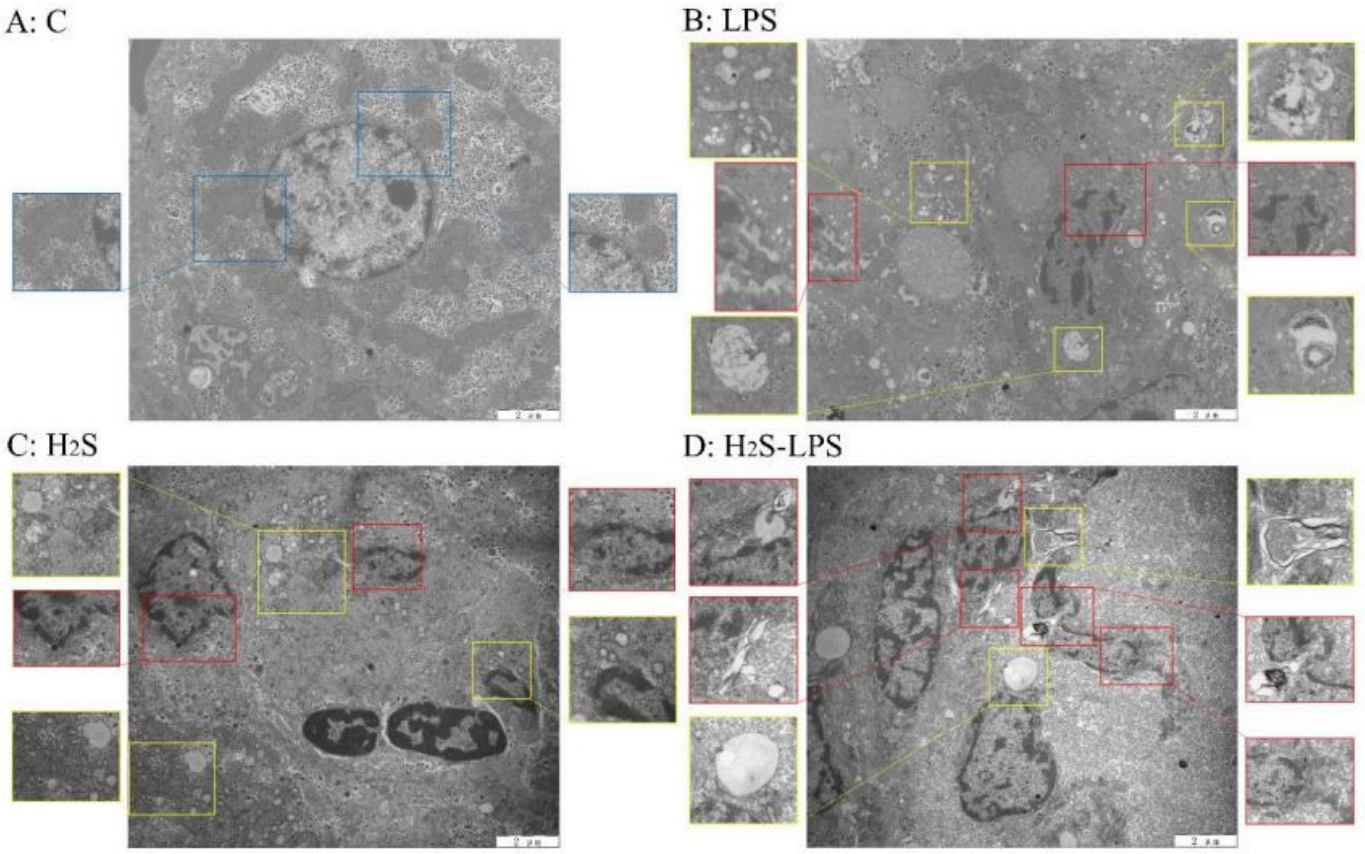

Figure 3

Ultrastructural observation of pathological changes in liver tissue. (A): C group; (B): H2S group; (C): LPS group; (D): H2S-LPS group. Fields from one representative experiment of three are shown (Scale bar, 2μm). Normal cell, and the nucleus was approximately round without obvious pathological changes (Blue boxes). Mitochondria swelled and vacuolated, holes formed on the cell membrane, cytoplasmic contents overflowed (Red boxes) and a large number of vacuoles (Yellow boxes).

Fig. 4

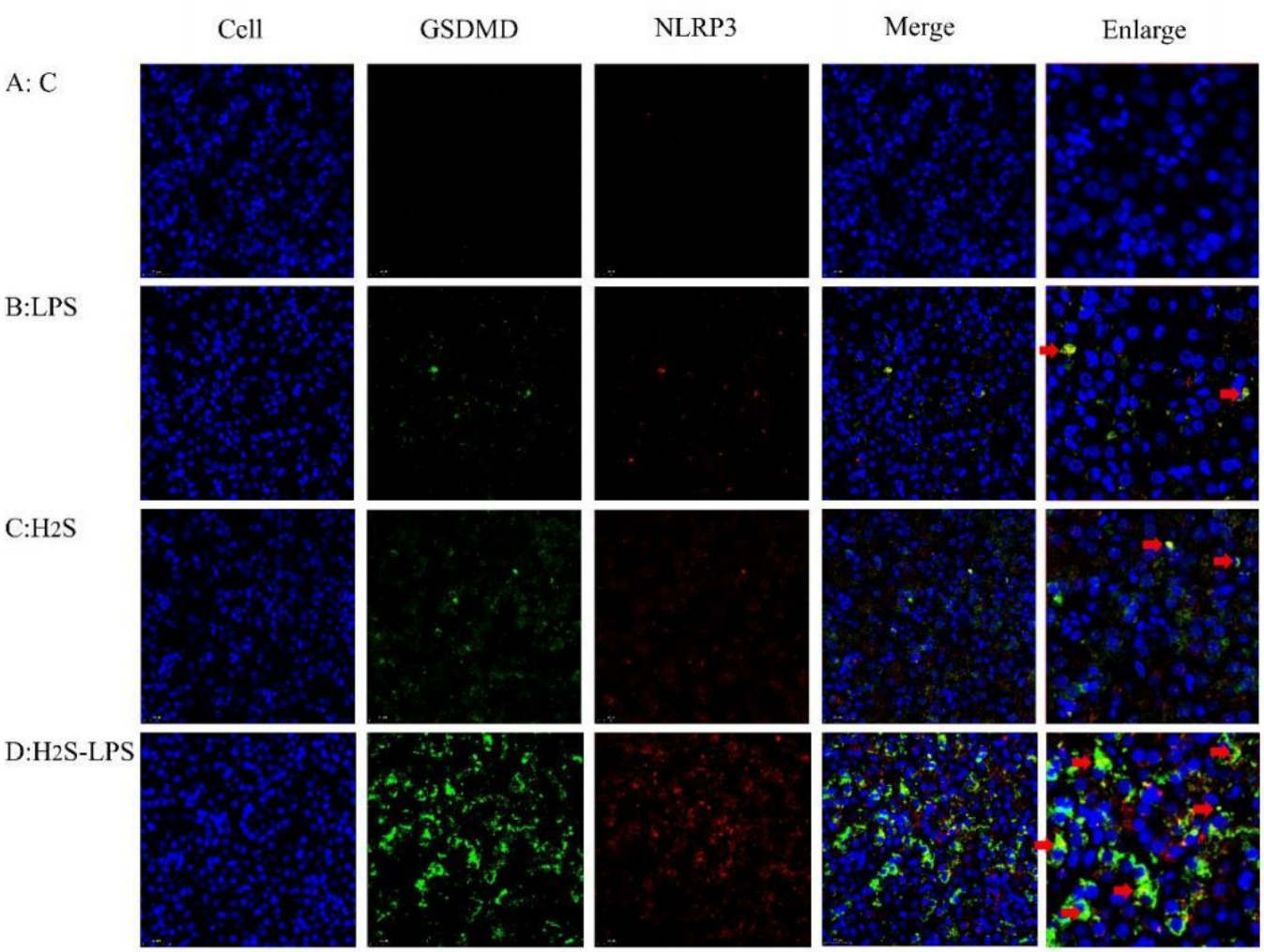

Figure 4

H2S exposure increased expression of NLRP3 and GSDMD in chicken liver Fluorescence staining analysis. (A): C group; (B): H2S group; (C): LPS group; (D): H2S-LPS group. Normal cell (Blue cells), GSDMD (Green cells) and NLRP3 (Red cells). Fields from one representative experiment of three are shown (Scale bar, 20μm).

Fig. 5

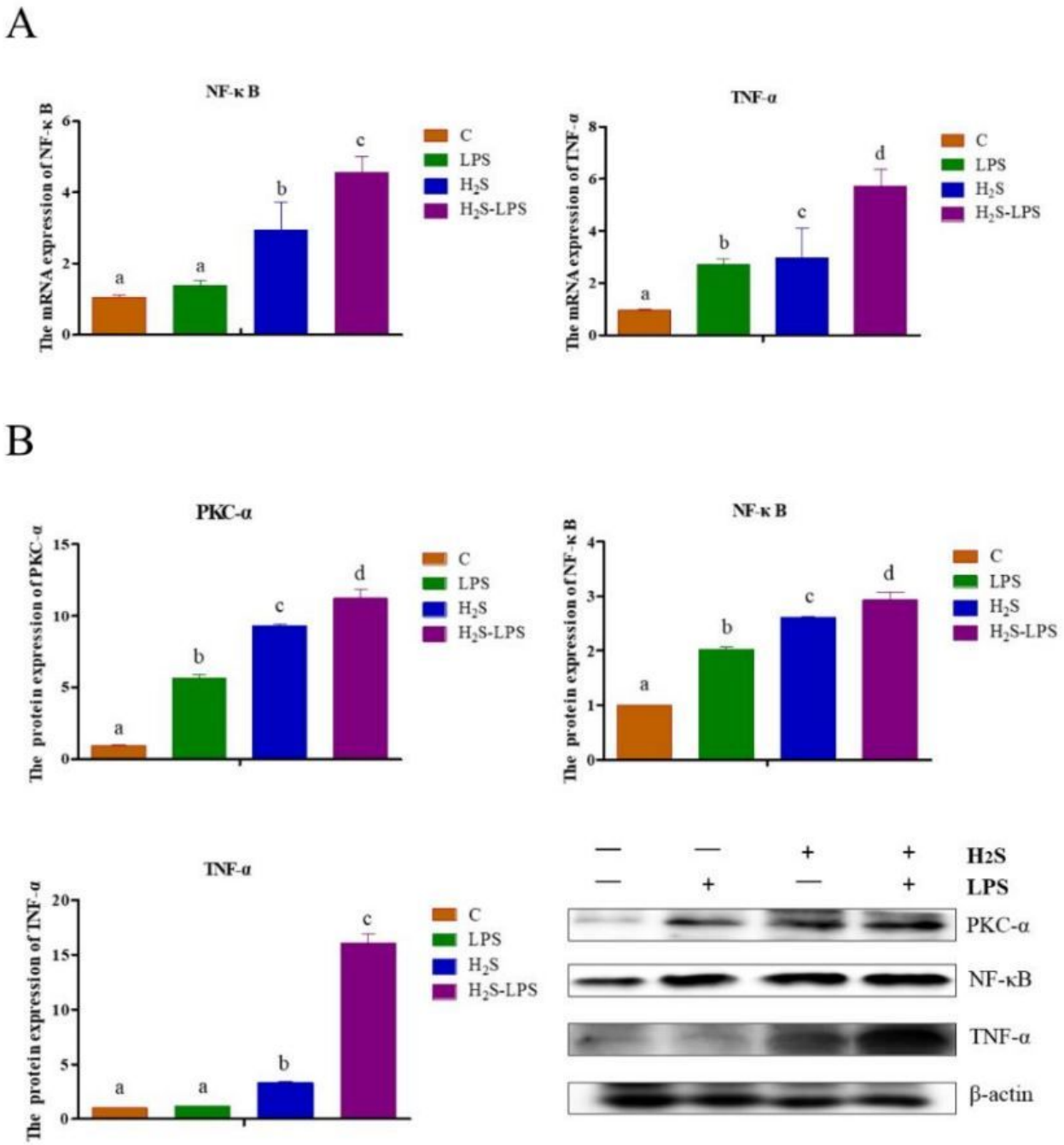

Figure 5

H2S induces chicken liver activated NF-κB/TNFα pathway (A): The mRNA expression level of NF-κB and TNFα. These results are from at least three independent experiments. There is a significant difference with the corresponding control ($P<0.05$). (B): The protein expression levels of PKCα, NF-κB and TNFα. These results are from at least three independent experiments. There is a significant difference with the corresponding control ($P<0.05$).

Fig. 6

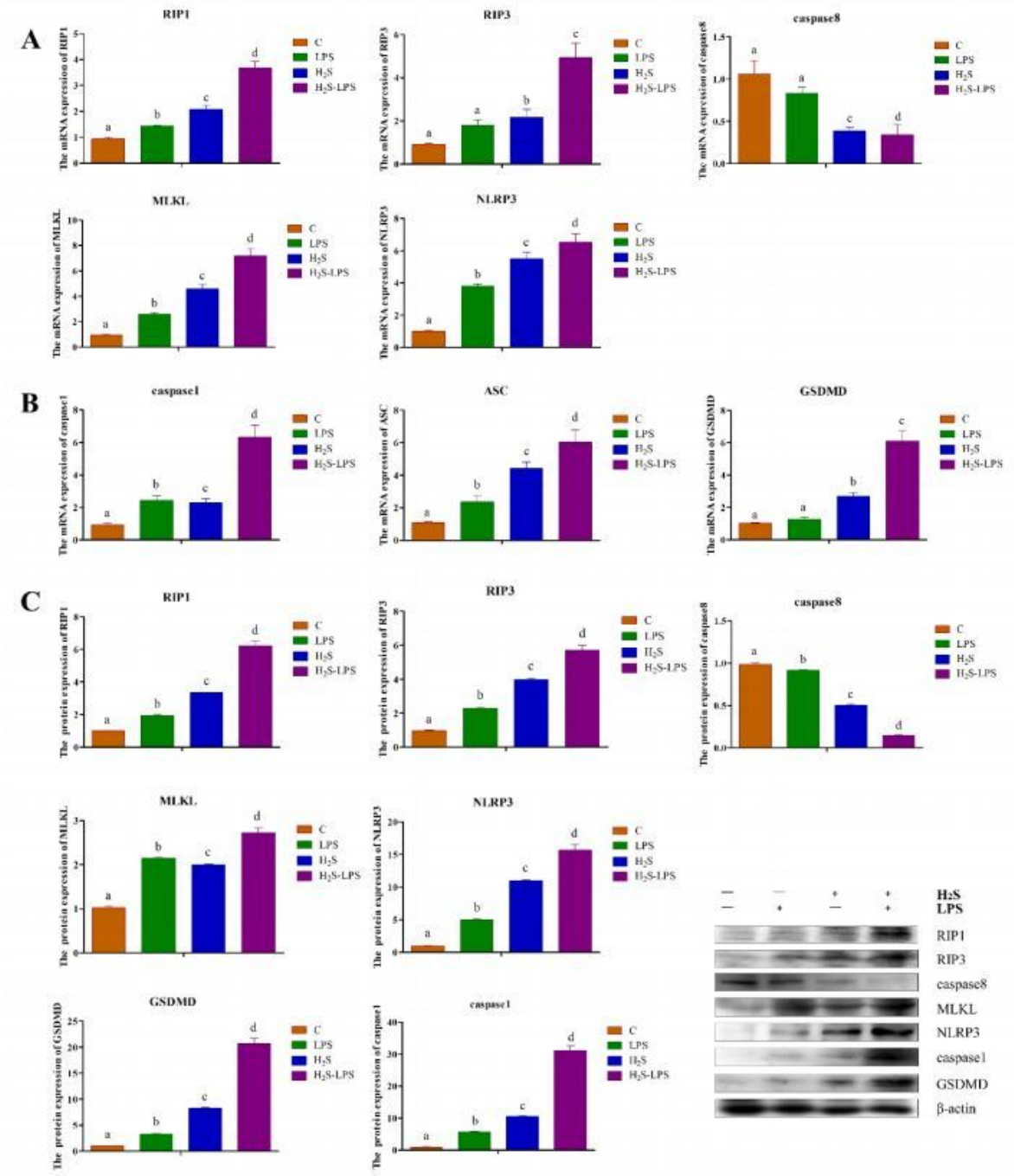

Figure 6

H2S induces chicken liver necrosis and pyroptosis (A): H2S exposure caused necrosis to liver tissue. The mRNA levels of necrosis factors in group C, H2S group, LPS group, and H2S-LPS group. There is a significant difference with the corresponding control ($P<0.05$). (B): H2S exposure caused liver tissue pyroptosis. The mRNA levels of key factors of pyroptosis in the group C, H2S group, LPS group, and H2S-LPS group. There is a significant difference with the corresponding control ($P<0.05$). (C): The protein

levels of necrosis and pyroptosis-related genes in the group C, H2S group, LPS group, and H2S-LPS group were significantly different from the corresponding controls (P<0.05).

Fig. 7

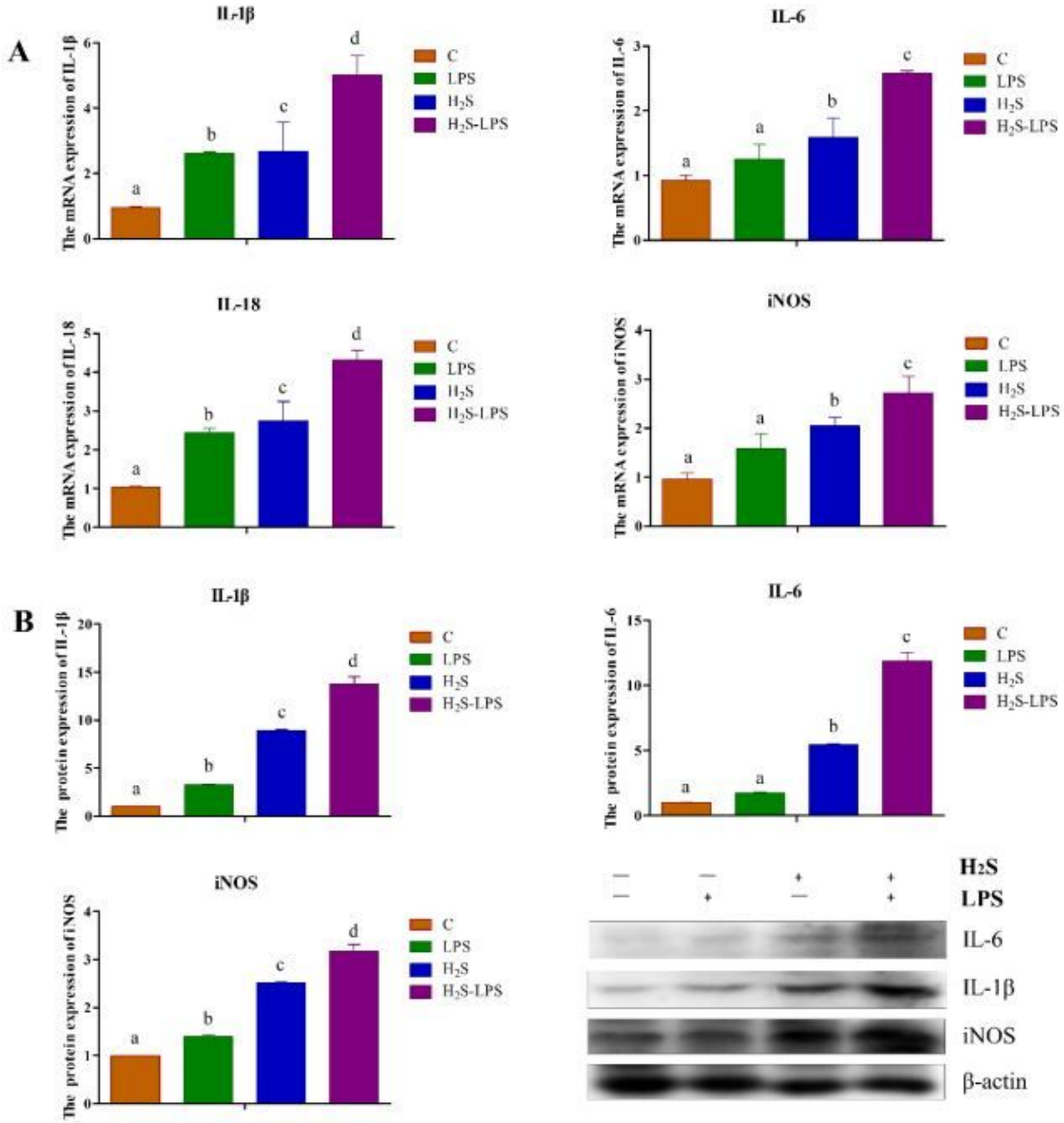

Figure 7

H2S exposure caused inflammatory damage f liver tissue. (A): The mRNA expression levels of inflammatory markers in group C, H2S group, LPS group, and H2S-LPS group. There is a significant difference with the corresponding control (P<0.05). (B): The protein expression levels of inflammatory

markers in group C, H2S group, LPS group, and H2S-LPS group. There is a significant difference with the corresponding control (P<0.05).

Fig. 8

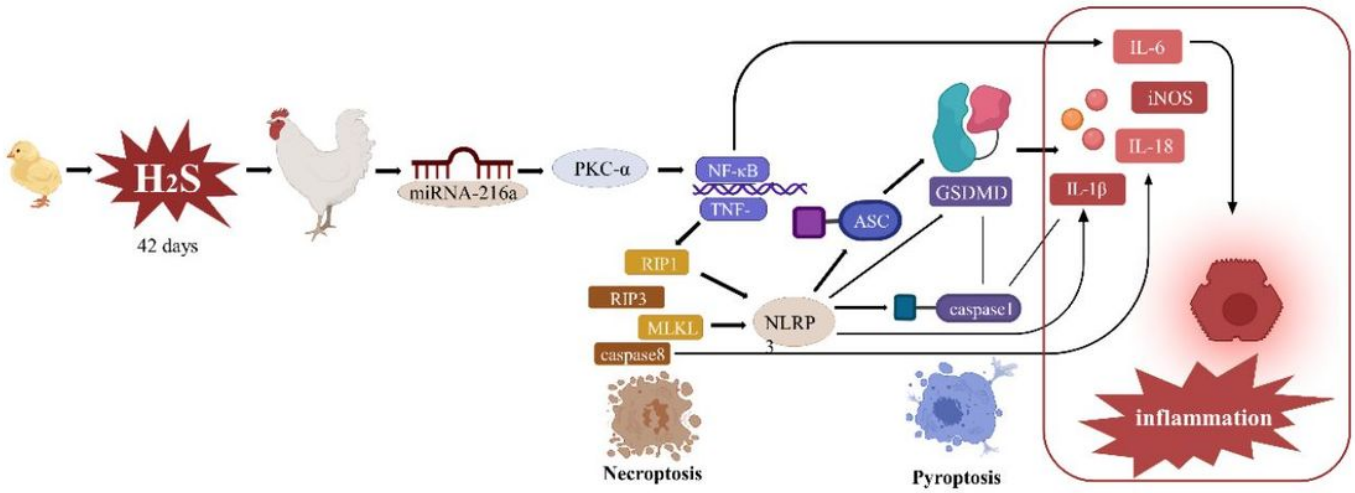

Figure 8

H2S exposure forms microRNA-216a / PKCα axis by targeting PKCα, activates NF-κB/TNFα pathway. H2S promotes the formation of necrosome in the liver, and further promotes the formation of pyroptosis bodies, which eventually leads to the release of inflammatory factors and causes inflammatory damage to the liver. At the same time, aggravated LPS-induced liver necrosis and pyroptosis, result in the aggravation of liver inflammation.

Supplementary Files

This is a list of supplementary files associated with this preprint. Click to download.

- Tables.pdf